

1 Revealing mechanisms of infectious 2 disease transmission through 3 empirical contact networks

4 Pratha Sah¹, Michael Otterstatter², Stephan T. Leu³, Sivan Leviyang⁴, Shweta
5 Bansal^{1*}

*For correspondence:

shweta.bansal@georgetown.edu
(SB)

6 ¹Department of Biology, Georgetown University, Washington, DC; ²British Columbia
7 Centre for Disease Control, Vancouver, Canada; ³Department of Biological Sciences,
8 Macquarie University, Sydney, Australia; ⁴Department of Mathematics, Georgetown
9 University, Washington, DC

11 Abstract

12 The spread of pathogens fundamentally depends on the underlying contacts between individuals.
13 Modeling infectious disease dynamics through contact networks is sometimes challenging,
14 however, due to a limited understanding of pathogen transmission routes and infectivity. We
15 developed a novel tool, INoDS (Identifying Network models of infectious Disease Spread) that
16 estimates the predictive power of empirical contact networks to explain observed patterns of
17 infectious disease spread. We show that our method is robust to partially sampled contact
18 networks, incomplete disease information, and enables hypothesis testing on transmission
19 mechanisms. We demonstrate the applicability of our method in two host-pathogen systems:
20 *Crithidia bombi* in bumble bee colonies and Salmonella in wild Australian sleepy lizard populations.
21 The performance of INoDS in synthetic and complex empirical systems highlights its role in
22 identifying transmission pathways of novel or neglected pathogens, as an alternative approach to
23 laboratory transmission experiments, and overcoming common data-collection constraints.

25 Introduction

26 Host contacts, whether direct or indirect, play a fundamental role in the spread of infectious
27 diseases (*Newman, 2002; Rohani et al., 2010; Bansal et al., 2007; Sah et al., 2017a*). Traditional
28 epidemiological models make assumptions of homogeneous social structure and mixing among
29 hosts which can yield unreliable predictions of infectious disease spread (*Shirley and Rushton, 2005;*
30 *Volz and Meyers, 2007; Bansal et al., 2007; Chen et al., 2014*). Network approaches to modeling the
31 spread of infectious diseases provide an alternative by explicitly incorporating host interactions that
32 mediate pathogen transmission. Formally, in a contact network model, individuals are represented
33 as nodes, and an edge between two nodes represents an interaction that has the potential to
34 transmit infection. Constructing a complete contact network model requires (i) knowledge about
35 the transmission routes of a pathogen, (ii) a sampling of all individuals in a population, and (iii) a
36 sampling of all disease-causing interactions among the sampled individuals. In addition, accuracy
37 of disease predictions depends on the quantification of the epidemiological characteristics of the
38 pathogen, including the rate of pathogen transmission given a disease-causing contact between
39 two individuals, and the rate of recovery of infected individuals.

40 The use of modern technology in recent years, including RFID, GPS, radio tags, proximity loggers

41 and automated video tracking has enabled the collection of detailed movement and contact data,
42 making network modeling feasible. Despite the technology, logistical and financial constraints
43 still prevent data collection on all individuals and their social contacts (*Welch et al., 2011; Cross*
44 *et al., 2012; Godfrey, 2013; Krause et al., 2013; Farine and Whitehead, 2015; Silk et al., 2015*). More
45 importantly, limited knowledge about a host-pathogen system makes it challenging to identify the
46 mode of infection transmission, define the relevant disease-causing contacts between individuals,
47 and measure per-contact rate of infection transmission (*Craft and Caillaud, 2011; White et al., 2015;*
48 *Manlove et al., 2017*). Laboratory techniques of unraveling transmission mechanisms usually take
49 years to resolve (*Velthuis et al., 2007; Aiello et al., 2016; Antonovics et al., 2017*). Defining accurate
50 contact networks underlying infection transmission in human infectious disease has been far from
51 trivial (*Bansal et al., 2007; Pellis et al., 2014; Eames et al., 2015*). For animal infectious disease,
52 limited information on host behavior and the epidemiological characteristics of the spreading
53 pathogen makes it particularly difficult to define a precise contact network, which has severely
54 limited the scope of network modeling in animal and wildlife epidemiology (*Craft and Caillaud,*
55 *2011; Craft, 2015*).

56 Lack of knowledge about disease transmission mechanisms has prompted the use of several
57 indirect approaches to identify the link between social structure and disease spread. A popular
58 approach has been to explore the association between social network position (usually quantified
59 as network degree) of an individual and its risk of acquiring infection (*Godfrey et al., 2009, 2010;*
60 *Leu et al., 2010; MacIntosh et al., 2012*). Another approach is to use proxy behaviors, such as
61 movement, spatial proximity or home-range overlap, to measure direct and indirect contact net-
62 works occurring between individuals (*Danon et al., 2011; Hamede et al., 2009; Fenner et al., 2011*).
63 A recent approach, called the *k*-test procedure, explores a direct association between infectious
64 disease spread and a contact network by comparing the number of infectious contacts of infected
65 cases to that of uninfected cases (*VanderWaal et al., 2016*). However, several challenges remain in
66 identifying the underlying contact networks of infection spread that are not addressed by these
67 approaches. First, it is often unclear how contact intensity (e.g. duration, frequency, distance) relate
68 to the risk of infection transfer unless validated by transmission experiments (*Aiello et al., 2016*).
69 Furthermore, the role of weak ties (i.e., low intensity contacts) in pathogen transfer is ambiguous
70 (*Pellis et al., 2014; Sah et al., 2017b*). The interaction network of any social group will appear as a
71 fully connected network if monitored for a long period of time. As fully-connected contact networks
72 rarely reflect the dynamics of infectious disease spread through a host population, one may ask
73 whether weak ties can be ignored, or what constitutes an appropriate intensity threshold below
74 which interactions are epidemiologically irrelevant? Second, many previous approaches ignore the
75 dynamic nature of host contacts. The formation and dissolution of contacts over time is crucial in
76 determining the order in which contacts occur, which in turn regulates the spread of infectious
77 diseases through host networks (*Bansal et al., 2010; Fefferman and Ng, 2007; Farine, 2017*). Finally,
78 none of the existing approaches allow direct comparison of competing hypotheses about disease
79 transmission mechanisms which may generate distinct contact patterns and consequently different
80 contact network models.

81 All of these challenges demand an approach that can allow direct comparison between com-
82 peting contact network models while taking into account the dynamics of host interactions and
83 data-constraints of network sampling. In this study, we introduce a computational tool called INoDS
84 (*I*dentifying *N*etwork models of infectious *D*isease *S*pread) that quantifies the predictive power
85 of empirical contact networks in explaining infectious disease spread, and enables comparison of
86 competing hypotheses about transmission mechanisms of infectious diseases. Our tool can also
87 infer the per-contact transmission rate of various infectious disease types (SI, SIS, and SIR), and
88 can be easily extended to incorporate other complex models of disease spread. The INoDS tool
89 provides inference on dynamic and static contact networks, and is robust to common forms of
90 missing data. Using two empirical datasets, we highlight the two-fold application of our approach –
91 (*i*) to identify whether observed patterns of infectious disease spread are likely given an empirical

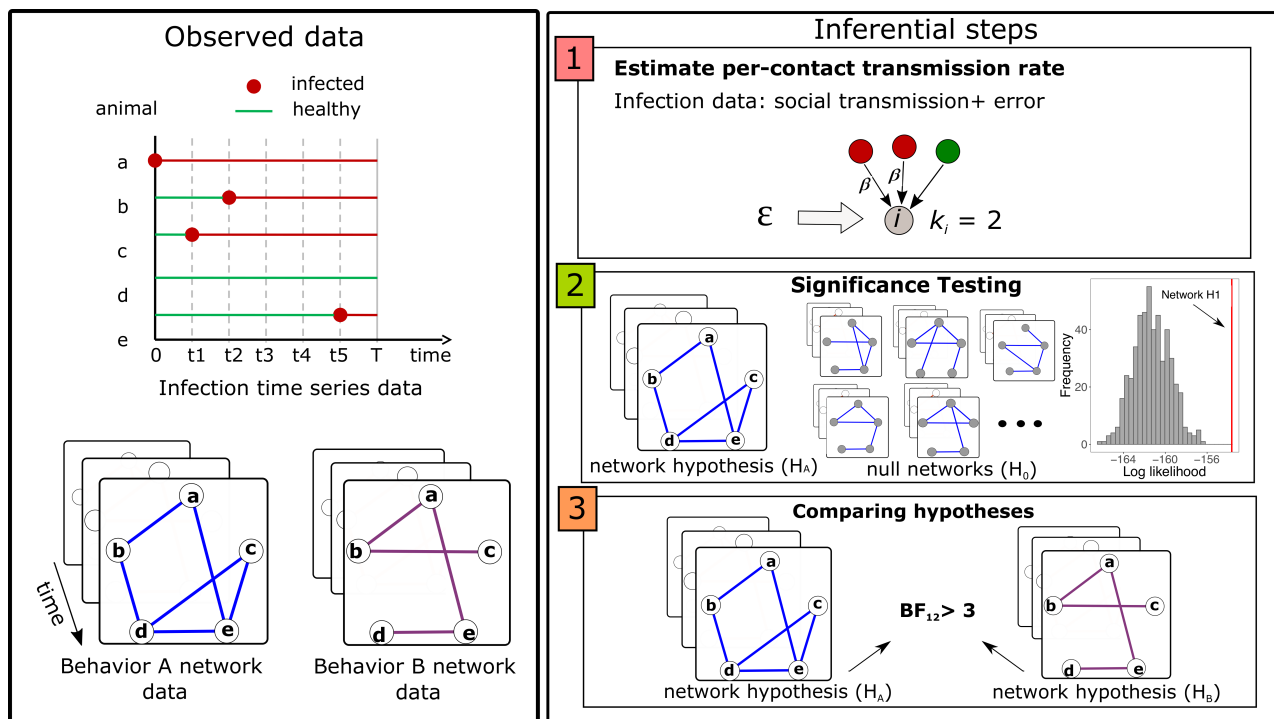


Figure 1. A schematic of our algorithm. **Observed data:** INoDS utilizes an observed infection time-series to estimate evidence towards a static or dynamic contact network hypothesis (or hypotheses) using a three step procedure. Shown here is an example of two competing contact network hypothesis based on different definitions of disease-causing contact (quantified by behavior A and behavior B). **Inferential steps:** In the first step, the tool estimates per-contact transmission rate parameter β , and an error parameter ϵ which captures the components of infection propagation unexplained by the edge connections of the network hypothesis. Second, the likelihood that the infectious disease spreads through the edge connections of the contact network hypothesis is compared to a distribution of likelihoods obtained from an ensemble of randomized networks. The predictive power of the empirical network hypothesis is considered to be high when its likelihood is higher than the null likelihood distribution at 5% significance level. Third, the marginal likelihood for the contact network hypothesis is calculated, which is then used to perform model comparison (using Bayes Factor, BF) between multiple contact network hypotheses, wherever available.

92 contact network, and (ii) to identify transmission routes, the role of the contact intensity, and the per
 93 contact transmission rate of a host-pathogen system. The epidemiological mechanisms of infection
 94 transmission identified by INoDS can therefore provide invaluable insights during implementation
 95 of immediate disease control measures in the event of an epidemic outbreak.

96 Results

97 The primary purpose of INoDS is to assess whether an empirical contact network is likely to generate
 98 an observed infection time-series from a particular host population. INoDS also provides epidemio-
 99 logical insights into the spreading pathogen by estimating the per-contact rate of transmission. In
 100 practice, the structure of a contact network model depends on the mode of infection transmission,
 101 and is sensitive to the amount of missing data on nodes and edges. The tool therefore treats
 102 empirically collected contact network models as network hypotheses, and facilitates hypothesis
 103 testing between different contact networks. The INoDS algorithm follows a three step procedure
 104 (Figure 1). First, the tool estimates a per-contact pathogen transmission rate (β) and an error
 105 parameter (ϵ). The β parameter quantifies the rate of pathogen transmission through each edge of
 106 the contact network, and the ϵ parameter quantifies components of infection transmission that are
 107 unexplained by the edge connections of the contact network. In the second step, the likelihood of
 108 the observed infection time-series under the network hypothesis and pathogen transmission rate
 109 is compared to the null likelihood distribution based on an ensemble of randomized networks. The
 110 randomized networks are generated by permuting the edge connections of the network hypothesis,

111 while controlling the number of nodes and edges present. We consider the network hypothesis
112 to have high predictive power if the likelihood of the infection time-series given the hypothesis is
113 higher than the null likelihoods at the 5% significance level. In the final step, the marginal (Bayesian)
114 evidence is calculated for the network hypothesis, which can be used to perform model selection
115 between multiple network hypotheses.

116 In the sections that follow, we evaluate the
117 accuracy of the tool in recovering the transmis-
118 sion parameter, β , and its robustness to missing
119 data (missing individuals, missing contacts and
120 missing infection cases). We further demonstrate
121 the application of INoDS by using two empirical
122 datasets: (i) spread of an intestinal pathogen in
123 bumble bee colonies, and (ii) salmonella spread
124 in Australian sleepy lizards.

125 INoDS performance

126 We evaluated the performance of INoDS on
127 multiple infection time-series data generated by
128 performing numerical simulations of infection
129 spread on a synthetic dynamic network, for a
130 wide range of pathogen transmission rates.

131 We found that INoDS accurately estimates the
132 true value of pathogen transmission rate, β , and
133 the accuracy is independent of the spreading rate
134 of the pathogen (Figure 2). The error param-
135 eter, ϵ , specified in the algorithm improves the
136 estimate of transmission rate when either the
137 network data or disease surveillance is incom-
138 plete (Appendix Figure 1). The estimated rate of
139 pathogen transmission is therefore accurate even
140 when substantial network or infection time-series
141 data is missing (Appendix Figure 2). The expected
142 value of ϵ is zero when all infection transmission
143 events are explained by the edge connections in
144 the contact network hypothesis (Figure 2). Values
145 greater than zero, on the other hand, indicate
146 unexplained transmission events due to either
147 missing or inaccurate data (Appendix Figure 2).

148 Next, we tested the performance of INoDS
149 in establishing the epidemiological relevance of
150 a hypothesized contact network against three potential sources of error in data-collection: (a)
151 incomplete sampling of individuals in a population (missing nodes); (b) incomplete sampling of
152 interactions between individuals (missing edges); and (c) infrequent health diagnosis of individuals
153 (missing cases). The performance of the tool was quantified in terms of a true positive rate (i.e., the
154 proportion of times an epidemiologically relevant contact network with missing data was correctly
155 distinguished as statistically significant from an ensemble of randomized networks with the same
156 amount of missing data) and a true negative rate (i.e., the proportion of times a network with the
157 same degree distribution as the epidemiologically relevant contact network, but with randomized
158 edge connections, was correctly classified as statistically insignificant). We found INoDS to be both
159 sensitive and specific (with a high true positive and true negative rate) across a range of missing
160 data scenarios (Figure 3). The true positive rate of the tool remains close to one even when as low

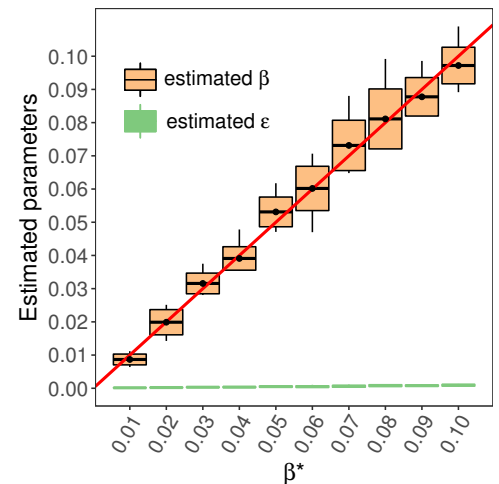


Figure 2. INoDS performance in recovering the per-contact pathogen transmission rate (β) for simulated infection time series under an susceptible-infected (SI) model. Each boxplot summarizes the results of 10 independent disease simulations; the black horizontal lines are the means of the estimated parameter values, the top and bottom black horizontal lines represent the standard deviation, and the tip of the black vertical line represents the maximum/minimum value. The solid red line represents one-to-one correspondence between the true value of the pathogen transmission rate (used to generate the simulated data), β^* , and the β value estimated by INoDS. Since the simulations were performed on a known synthetic network, the expected value of the error parameter, ϵ , (represented by the green lines) is zero.

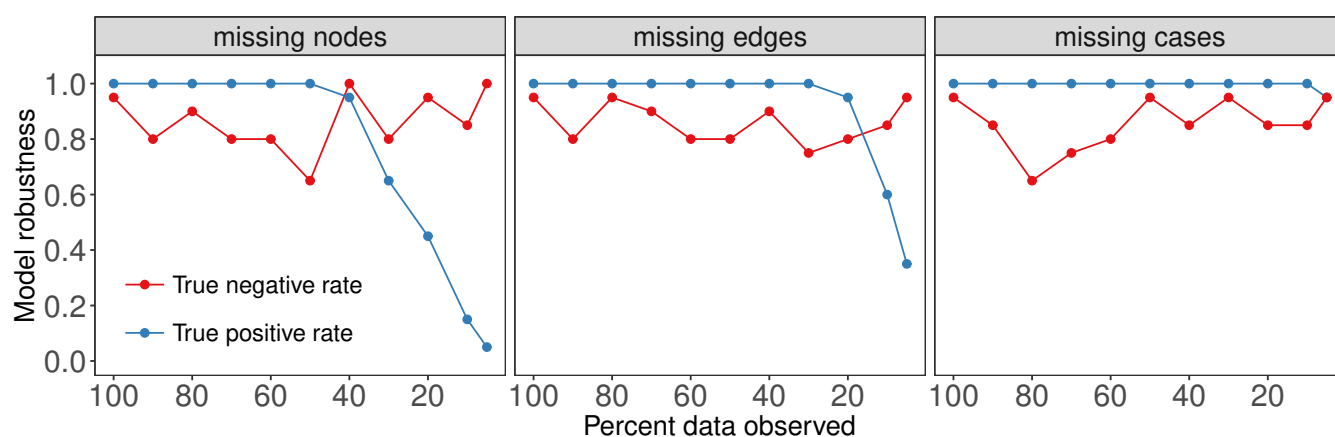


Figure 3. Robustness of INoDS in establishing the epidemiological significance of a hypothesized contact network under three common forms of missing data - missing nodes, missing edges and missing infection cases. True positive rate is calculated as the proportion of times ($n = 20$) the epidemiologically relevant (true) dynamic network was detected as statistically significant relative to a null distribution of randomized networks. True negative rate is calculated as the proportion of times ($n = 20$) a network with similar degree distribution as the epidemiologically relevant network, but randomized edge connections, was identified as statistically indistinguishable from the null distribution. The null distribution for a network hypothesis was generated by permuting all its edge connections, but preserving the number of nodes and edges.

Figure 3-Figure supplement 1. Robustness plot of (A) INoDS, (B) k -test and (C) network position test to three common forms of missing data - missing nodes, missing edges and missing infection cases. The null expectation in INoDS and the network position test was generated by permuting network edges, creating an ensemble of null networks. In the k -test, the location of infection cases within the observed network are permuted, creating a permuted distribution of the k -statistic (VanderWaal et al., 2016).

161 as 10% of infection cases are documented (missing cases, Figure 3). For incompletely sampled
 162 contact networks, the true positive rate remains close to one when at least 50% nodes or 30%
 163 edges are documented.

164 The performance of INoDS in discriminating the epidemiological contact network from null
 165 network hypotheses also surpasses two previous approaches - the k -test procedure and the
 166 network position test (Figure 3 - figure supplement). In comparison to INoDS, the k -test and
 167 network position test are sensitive to all three types of missing data. The true positive rate of the
 168 k -test declines with an increasing number of missing nodes, edges, or infection cases. Of the three
 169 approaches, the network position test has the lowest sensitivity (true positive rate). Since the k -test
 170 procedure and network position test have been primarily used in the context of non-dynamic
 171 networks, we repeated this analysis with simulated disease data from a static synthetic network.
 172 Appendix Figure 4 demonstrates that even for observed networks that are not dynamic, INoDS has
 173 greater sensitivity and specificity than the k -test procedure and the network position test.

174 Applications to empirical data-sets

175 We next demonstrate the application of INoDS to perform hypothesis testing on contact networks,
 176 identify transmission mechanisms and infer transmission rate using two empirical datasets. The first
 177 dataset is derived from the study by Otterstatter and Thomson (2007) that examined the spread of
 178 an intestinal pathogen (*Crithidia bombi*) within colonies of the social bumble bee, *Bombus impatiens*.
 179 The second dataset documents the spread of *Salmonella enterica* within two wild populations of
 180 Australian sleepy lizards *Tiliqua rugosa* Bull et al. (2012).

181 Determining transmission mechanism and the role of contact intensity: case study 182 of *Crithidia bombi* in bumble bees

183 Otterstatter and Thomson (2007) showed that the transmission of *C. bombi* infection in bumble
 184 bee colonies was associated with the frequency of contacts with infected nest-mates rather than
 185 the duration of contacts. However, the dynamic contact network models had a small number of

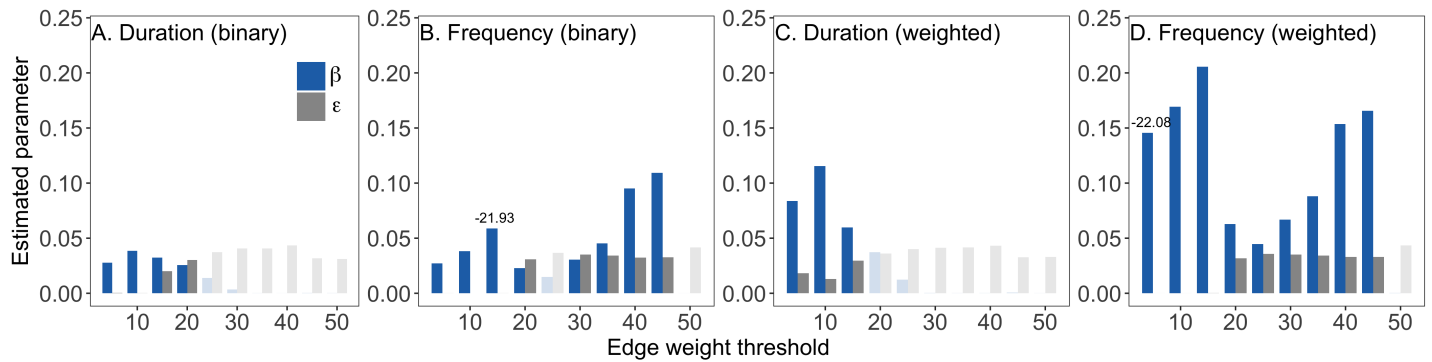


Figure 4. Identifying the contact network model of *Crithidia* spread in bumble bee colony (colony UN2). Edges in the contact network models represent physical interaction between the bees. Since the networks were fully connected, a series of filtered contact networks were constructed by removing weak weighted edges in the network. The x-axis represents the edge weight threshold that was used to remove weak edges in the network. Two types of edge weights were tested - duration and frequency of contacts. In addition, across all ranges of edge weight threshold, the weighted networks were converted to binary networks. The results shown are estimated values of the per contact rate transmission rate β , and estimated values of error ϵ , for the (A-B) the two types of binary network, (C) contact duration weighted network, (D) contact frequency weighted network. The faded bars correspond to networks where β parameter is statistically insignificant. Numbers above bars indicate the log Bayesian (marginal) evidence of the networks that were detected to have statistically significant higher predictive power as compared to an ensemble of null networks ($P < 0.05$, corrected for multiple comparisons).

186 nodes, and were fully connected (i.e., all individuals were connected to each other in the network) at
 187 all time steps. Because predictions of infection transmission is sensitive to the size and edge density
 188 of the contact network model, we extended the previous analysis by answering three specific
 189 questions: (1) Do physical contact networks have higher predictive power to explain the spread of
 190 *C. bombi* than random networks?, (2) Do the value of contact intensities (edge weights) matter in
 191 transmission?, and (3) Do weak ties between individuals contribute to infection transfer? To validate
 192 our tool, we performed analyses on two types of contact network models – those described by
 193 frequency of contacts and those described by duration of contacts – and compared the results with
 194 the findings reported in (Otterstatter and Thomson, 2007).

195 To answer the three questions, we constructed dynamic contact networks where edges represent
 196 close proximity between individuals. Since fully connected networks rarely describe the dynamics of
 197 infection spread, we sequentially removed edges with weights less than 10-50% of the highest edge
 198 weight to generate contact network hypotheses at different edge weight thresholds. Corresponding
 199 to the two types (frequency and duration) of weighted networks, unweighted contact networks
 200 were also constructed by replacing weighted edges in the thresholded weighted networks with
 201 binary edges (i.e., edges with an edge weight of one).

202 Figure 4 shows the estimates of pathogen transmission rate β , and error ϵ for the four types of
 203 contact network hypotheses at different edge weight thresholds. Only a subset of contact network
 204 hypotheses had statistically significant estimates of β (non faded bars). Two network hypotheses
 205 summarizing frequency of contacts – binary frequency network at 15% edge weight threshold
 206 and weighted frequency network at 5% edge weight threshold – demonstrated higher predictive
 207 power than an ensemble of null networks. Of the two, the weighted frequency network had slightly
 208 higher Bayesian evidence, although the binary frequency network was equally supported. In a
 209 separate colony (UN1), only the weighted frequency network at 5% edge weight threshold had
 210 higher predicted power compared to an ensemble of null networks (Appendix Figure 5). Together,
 211 our results therefore show that (1) contact networks capturing frequency (but not duration) of
 212 contacts have statistically high predictive power to explain the spread of *C. bombi* in bumble bee
 213 colonies, (2) the contact networks should be weighted, and (3) weak ties (i.e., edges with weights
 214 less than 5% of the highest weighted edge) are epidemiologically unimportant.

215 **Identifying transmission mechanisms with imperfect disease data: case study of**
216 ***Salmonella enterica* Australian sleepy lizards**

217 Spatial proximity is known to be an important factor in the transmission of *Salmonella enterica*
218 within Australian sleepy lizard populations (*Bull et al., 2012*). However, it is not known whether
219 the transmission risk increases with frequency of proximate encounters between infectious and
220 susceptible lizards. We therefore tested two contact network hypotheses to explain the spread
221 of salmonella at two sites of wild sleepy lizards populations. The first contact network hypothesis
222 placed binary edges between lizards if they were ever within 14m distance from each other during a
223 day (24 hours). We constructed the second contact network by assigning edge weights proportional
224 to the number of times two lizards were recorded within 14m distance of each other during a day.

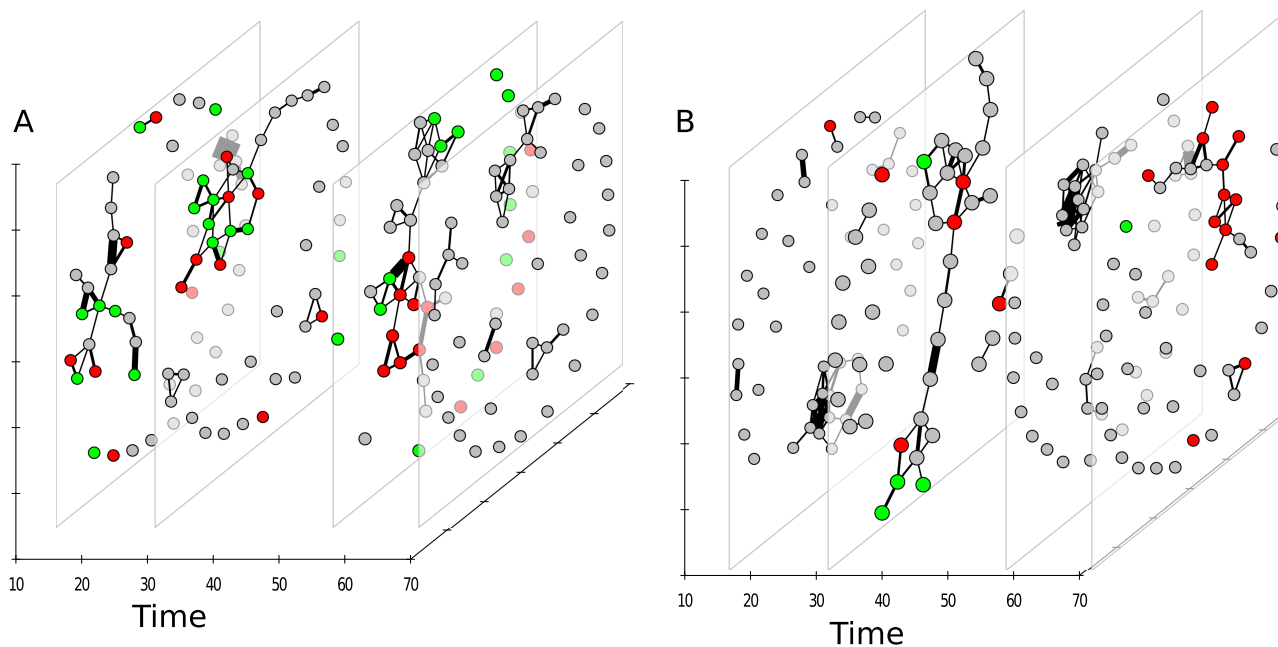
225 Because disease sampling was performed at regular fortnightly intervals, the true infection
226 time (day) of individuals at both study sites was unknown. We therefore used a data augmentation
227 method in INoDS (see Methods) to sample unobserved infection timings along with the per contact
228 transmission rate, β , and error, ϵ . We found that the likelihood of salmonella infection spreading
229 through the weighted contact network was significantly greater than the null expectation at both
230 sites (Figure 5). Compared to unweighted networks, networks with edges weighted by contact
231 frequency had higher marginal (Bayesian) evidence at both sites. This indicates that the occurrence
232 of repeated contacts between two spatially proximate individuals, rather than just the presence of
233 contact between individuals is important for *Salmonella* transmission.

234 **Discussion**

235 Network modeling of infectious disease spread is becoming increasingly popular, because modern
236 technology has dramatically improved the quality of data that can be collected from animal popula-
237 tions. However, the concepts of power analysis and hypothesis testing are still underdeveloped
238 in network modeling, even though such approaches are widely recognized as key elements to
239 establish how informative and appropriate a model is (*Jennions and Møller, 2003; Johnson et al.,*
240 *2015*). Our ability to define a contact network relies on our understanding of host behavior, and
241 the dominant transmission mode for a given pathogen. Since such information is either derived
242 from expert knowledge (which can be subjective) or laboratory experiments (which are time- and
243 resource-intensive), it is essential to conduct an a priori analysis of contact network models to avoid
244 uninformative or misleading disease predictions.

245 In this study we therefore present INoDS as a tool that performs network model selection and
246 establishes the predictive power of a contact network model to describe the spread of infectious
247 diseases. Our method also provides epidemiological insights about the host-pathogen system
248 by enabling hypothesis testing on different transmission mechanisms, and estimating pathogen
249 transmission rates (transmission parameter, β). Unlike previous approaches, our method is robust
250 to missing network data, imperfect disease surveillance, and can provide network inference for a
251 range of disease spread models. The tool can thus be used to provide inference on contact networks
252 for a variety of pathogen types occurring both in wildlife and human populations. Inferring the role
253 of dynamic contacts on infectious disease spread requires the knowledge of either order or timing
254 of infection of individuals in the network. In practice, constraints on data collection (e.g., due to
255 infrequent health assessments), or infection diagnostics (e.g., due to sub-clinical infection, poor
256 diagnostics) precludes precise knowledge of infection timing. To overcome this challenge, our tool
257 assumes the infection times in a host population to be unobserved, and uses data on infection
258 *diagnosis* instead to provide inference on contact networks.

259 Our work thus addresses a growing subfield in network epidemiology that leverages statistical
260 tools to infer contact networks using all available host and disease data (*Welch et al., 2011; Stack*
261 *et al., 2013; VanderWaal et al., 2016; Groendyke et al., 2011*). Our approach can be used to tackle
262 several fundamental challenges in the field of infectious disease modeling (*Eames et al., 2015;*
263 *Pellis et al., 2014*). First, INoDS can be used to perform model selection on contact network models



Site	Transmission mechanism	β	ϵ	Predictive power	Evidence
Site 1	Direct transmission, binary	0.011	0.034	0.03	-1019.33
Site 1	Direct transmission, weighted (frequency) *	0.376	0.037	0.03	-219.44
Site 2	Direct transmission, binary	0.061	0.042	0.15	-775.80
Site 2	Direct transmission, weighted (frequency) *	2.734	0.075	<0.001	-250.61

Figure 5. Identifying transmission mechanisms of *Salmonella* spread in Australian sleepy lizards. Dynamic network of proximity interactions for a total duration of 70 days between (A) 43 lizards at site 1, and (B) 44 lizards at site 2. Each temporal slice summarizes interactions within a day (24 hours). Edges indicate that the pair of individuals were within 14m distance of each other, and the edge weights are proportional to the frequency of physical interactions between the node pair. Green nodes are the animals that were diagnosed to be uninfected at that time-point, red are the animals that were diagnosis to be infected and grey nodes are the individuals with unknown infection status at the time-point. We hypothesized that the spatial proximity networks could explain the observed spread of *Salmonella* in the population. The results are summarized as a table. Bold numbers indicate that the network hypothesis was found to have high predictive power compared to an ensemble of randomized networks. The network hypothesis with the highest log Bayesian (marginal) evidence at each site is marked with an asterisk (*)

264 that quantify different transmission modes; this approach therefore facilitates the identification
265 of infection-transmitting contacts and does not rely on laboratory experimentation (or subjective
266 expert knowledge). Second, INoDS can be used to establish the predictive power of proxy measures
267 of contact in cases where limited interaction data is available. For example, spatial proximity,
268 home-range overlap or asynchronous refuge use are commonly used as a proxy for disease-causing
269 contact in wild animal populations (*Godfrey et al., 2010; Leu et al., 2010; Sah et al., 2016*). INoDS
270 establishes the epidemiological significance of such assumptions by comparing the likelihood
271 of infection spread occurring along the edges of the proxy contact network to the likelihoods
272 generated from an ensemble of random networks. Third, it is well known that not all contacts
273 between hosts have the same potential for infection transmission. The heterogeneity of host
274 contacts in a network model is typically captured through edge weights, but it is often not clear
275 which type of edge weights (frequency, duration or intensity) is relevant in the context of a specific
276 host pathogen system (*Pellis et al., 2014*). Through model selection of contact networks with similar
277 edge connection but different edge weighting criterion, INoDS can help establish a link between
278 edge weight and the risk of transmission across an edge in a contact network.

279 We demonstrate the application of INoDS using two real-world datasets. In the first dataset, we
280 used INoDS to determine the role of edge weight type and edge weight value on the predictive
281 power of the contact network. To accurately model the spread of the *Crithidia* gut protozoan in
282 bumble bee colonies, we show that the contact networks weighted with respect to frequency,
283 rather than duration, have higher predictive power given observed patterns of transmission. Our
284 results therefore support the original finding of the study (*Otterstatter and Thomson, 2007*), where
285 individual risk of infection was found to be correlated with contact rate with infected nest-mates.
286 Our analysis further extends previous findings in this system by comparing the observed patterns
287 of transmission against null expectations from random networks, and assessing the likelihood
288 of competing network hypotheses. We find weak ties below a certain threshold do not play an
289 important role in infection transfer. Contact networks where such weak weighted edges have
290 been removed, therefore, demonstrate higher predictive power than fully connected networks. In
291 the next empirical example, we explore the transmission mechanisms of a commensal bacterium
292 in wild populations of Australian sleepy lizards. We find that taking repeated contacts between
293 closely located lizards into account allows better, i.e. more consistent, predictions on Salmonella
294 transmission.

295 The current version of INoDS assumes the infection process has no latent period, and that the
296 infectiousness of infected hosts and susceptibility of naive hosts is equal for all individuals in the
297 population. These assumptions can be relaxed to incorporate more complex disease progression.
298 For instance, heterogeneity in infectiousness of infected hosts and the susceptibility of naive
299 hosts can be incorporated as random effects in the model by assuming the two follow a Gaussian
300 distribution. Disease latency can also be incorporated using a data-augmentation technique, similar
301 to what we use for inferring infection times.

302 Our results show that the data-collection efforts should aim to sample as many individuals in
303 the population as possible, since missing nodes have the greatest impact (rather than missing
304 edges) on the predictive power of network models. Since data-collection for network analysis can be
305 labor-intensive and time-consuming, our approach can be used to make essential decisions on how
306 limited data collection resources should be deployed. Our approach can also be used to improve
307 targeted disease management and control by identifying high-risk behaviors and super-spreaders
308 of a novel pathogen without relying on expensive transmission experiments that take years to
309 resolve.

310 **Methods**

311 Here we describe INoDS, a computational tool that (i) estimates per contact transmission rate (β)
312 of infectious disease for empirical contact networks, (ii) establishes predictive power of a contact
313 network by comparisons with an ensemble of randomized networks, and (iii) enables discrimination

314 of competing contact network hypotheses, including those based on pathogen transmission mode,
 315 edge weight criteria and data collection techniques. Two types of data are required as input for
 316 INoDS – infection time-series data, which include infection diagnoses (coded as 0 = not infected and
 317 1 = infected), and time-step of diagnosis for all available individuals in the population; and an edge-
 318 list of a dynamic (or static) contact network. An edge-list format is simply the list of node pairs (each
 319 node pair represents an edge of the network), along with the weight assigned to the interaction, and
 320 time-step of interaction, with one node pair per line. The tool can be used for unweighted contact
 321 networks - an edge weight of one is assigned to all edges in this case. Time-steps of interactions are
 322 not required when analysis is performed on static contact networks. The software is implemented in
 323 Python, is platform independent, and is freely available at <https://bansallab.github.io/INoDS-model/>.

324 INoDS formulation

325 We assume that at each instance the potential of acquiring infection for a susceptible individual i
 326 depends on the per contact transmission rate β , the total strength of interactions with its infected
 327 neighbors at the previous time-step, and an error parameter ϵ that captures the force of infection
 328 that is not explained by the individual's social connections. The infection receiving potential, $\lambda_i(t_i)$,
 329 of individual i at time t is thus calculated as:

$$\lambda_i(t) = 1 - \exp\{-\beta w_i(t-1) - \epsilon\}, \quad (1)$$

330 where both transmission rate β and error parameter ϵ are > 0 ; $w_i(t-1)$ denotes the total strength
 331 of association between the focal individual i and its infected associates at the previous time-step
 332 ($t-1$). For binary (unweighted) contact network models $w_i = k_i$, where k_i is the total infected
 333 connections of the focal individual.

334 The log-likelihood for all observed timings of infection in a population given the contact network
 335 hypothesis (H_A) can therefore be estimated as:

$$\log(D|H_A, \beta, \epsilon) = \sum^n \log[\lambda_n(t_n)] + \sum^t \left(\sum^m \log[1 - \lambda_m(t)] \right), \quad (2)$$

336 where t_n is the time of infection of individual n . The first part of equation 2 estimates the log
 337 likelihood of all observed infection acquisition events. The second part of the equation represents
 338 the log-likelihood of susceptible individuals m remaining uninfected at time t .

339 Parameter estimation and data augmentation of infection timings

340 We adopted a Bayesian MCMC framework to estimate the unknown model parameters. Calculation
 341 of the likelihood in equation 2 requires knowledge of exact timing of infection, t_1, \dots, t_n , for n infected
 342 individuals in the population. However in many cases, the only data that is available are the timings
 343 of when individuals in a populations were *diagnosed* to be infected, d_1, \dots, d_n . We therefore employ
 344 a Bayesian data augmentation approach to estimate the actual infection timings in the disease
 345 dataset (*Tanner and Wong, 1987*). Since in this case the actual infection time t_i for an individual i is
 346 unobserved, we only know that the timing of infection for the individual lies between the interval
 347 (L_i, d_i], where L_i is the last negative diagnosis of individual i before infection acquisition. Within this
 348 interval, the individual could have potentially acquired infection at any time-step where it was in
 349 contact with other individuals in the network. Assuming incubation period to be one time-step, we
 350 can therefore represent the potential set of infection timings as $t_i \in \{g_i(t_i-1) > 0, L_i < t_i \leq d_i\}$, where
 351 $g_i(t_i-1)$ is the degree (number of contacts) of individual i at time t_i-1 . For infections that follow a
 352 SIS or SIR disease model, it is also essential to impute the recovery time of infected individuals for
 353 accurate estimation of infected degree. To do so, we adopt a similar data augmentation approach
 354 as described to sample from the set of possible recovery time-points.

355 The joint posterior distribution of augmented data and the set of parameters is proportional to:

$$P(\Theta|D, H) = \frac{\mathcal{L}(D|H, \Theta)\mathcal{P}(\Theta|H)}{\mathcal{E}(D|H)} \propto \mathcal{L}(D|H, \Theta)\mathcal{P}(\Theta|H) \quad (3)$$

356 where D is the infection time-series data, H is the contact network hypothesis, and $P, \mathcal{L}, \mathcal{P}, \mathcal{E}$
357 are the shorthands for the posterior, the likelihood, the prior and the evidence, respectively. The
358 data augmentation proceeds in two steps. In the first step, the missing infection times are imputed
359 conditional on the possible set of infection times. In the next step the posterior distributions of the
360 unknown parameters are sampled based on the imputed data. We performed data imputation
361 using inverse transform sampling method, which is a technique of drawing random samples from
362 any probability distribution given its cumulative distribution function (*Robert and Casella, 2004*).
363 We used a uniform prior on $[0, 1000]$ for the per contact transmission rate and the error
364 parameter.

365 MCMC sampling of the unknown parameters is performed using the *PTsampler* function of *emcee*
366 package implemented in Python (*Foreman-Mackey et al., 2013*). *PTsampler* is an implementation
367 of the affine-invariant ensemble MCMC algorithm which provides efficient sampling of highly cor-
368 related parameters - a common problem when using simple Metropolis-Hastings type samplers
369 (*Foreman-Mackey et al., 2013*). INoDS uses twice the number of walkers as the total model pa-
370 rameters, and the temperature is set to $T = 15$ to maximize the sampling of the parameter space.
371 The values of The number of sampling steps and burn-in is specified by the user. Convergence is
372 assessed using an autocorrelation plot of few randomly selected walkers. From the joint posterior
373 estimates of β and ϵ , we report the parameter combination with the highest maximum likelihood
374 value.

375 **Statistical significance of infection transmission parameter**

376 The statistical significance of parameter β is determined by comparing the force of infection
377 explained by edge connections ($=\beta w_i(t-1)$) at each infection event to the error parameter ϵ . The
378 p -value is calculated as the proportion of transmission events where the force of infection is greater
379 than the error estimate. The per contact transmission rate β is considered to be statistically
380 significant when its calculated p -value is less than 0.05.

381 **Interpretation of the error parameter**

382 In principle, inclusion of the error parameter in eq. 1 is similar to the asocial learning rate used in
383 the network based diffusion analysis approach in the behavior learning literature (*Franz and Nunn,*
384 *2009; Aplin et al., 2013*). However, in contrast to the asocial learning rate which quantifies the
385 rate of spontaneous learning, ϵ in INoDS formulation serves to improve the estimation of the per
386 contact transmission rate, β , when either the contact network or infection spread is not completely
387 sampled (Appendix Figure 1 and 2). The magnitude of ϵ can also be used to (approximately)
388 assess the magnitude of missing data (Appendix Figure 3). The percentage transmission events
389 where ϵ is greater than the force of infection explained by edge connections ($=\beta w_i(t-1)$) increases
390 proportionately with increasing amount of missing network data. The relative differences between
391 social force of infection and unexplained transmission events, however is less sensitive to missing
392 data on infection cases.

393 **Predictive power of a contact network hypothesis**

394 We assess the predictive power of a contact network hypothesis by performing comparisons
395 with an ensemble of randomized networks with same number of nodes and edge connectivity.
396 Specifically, the likelihood of the infection data given the network and estimated model parameters
397 (i.e., $\mathcal{L}(D|H, \Theta)$) is compared to a distribution of likelihoods of infection data (given the estimated
398 model parameters) obtained from the null networks (i.e., $\mathcal{L}(D|H_{O_1}, \Theta), \mathcal{L}(D|H_{O_2}, \Theta), \dots, \mathcal{L}(D|H_{O_n}, \Theta)$;
399 $n = 500$). Null networks are generated by randomizing edge connections of the contact network
400 hypothesis, which preserves the edge density in the permuted networks. Next, a p -value is calculated
401 as the proportion of randomizations which generate a likelihood greater than the likelihood of
402 the empirical network hypothesis. The empirical contact network is considered to have a higher
403 predictive power than the null expectation when its calculated p -value is less than 0.05.

404 **Model selection of competing network hypotheses**

405 To facilitate model selection in cases where there are more than one network hypothesis, we
406 compute the marginal likelihood of the infection data given each contact network model. The
407 marginal likelihood, also called the Bayesian evidence, measures the overall model fit, i.e., to what
408 extent the infection time-series data can be simulated by a network hypothesis (H_A). Bayesian
409 evidence is based on the average model fit, and calculated by integrating the model fit over the
410 entire parameter space:

$$P(D|H) = \int \mathcal{P}(\Theta|H)\mathcal{L}(D|H, \Theta)d\Theta \quad (4)$$

411 Since it is difficult to integrate Eq.4 numerically, we estimate the marginal likelihood of network
412 models using thermodynamic integration, or path sampling (*Lartillot and Philippe, 2006*) method
413 implemented in *emcee* package in Python. Model selection can be then performed by computing
414 pair-wise Bayes factor, i.e. the ratio of the marginal likelihoods of two network hypotheses. The log
415 Bayes factor to assess the performance of network hypothesis H_A over network hypothesis H_B , is
416 expressed as:

$$\log(B_{BA}) = \log(P(D|H_B)) - \log(P(D|H_A)) \quad (5)$$

417 The contact network with a higher marginal likelihood is considered to be more plausible, and
418 a log Bayes' factor of more than 3 is considered to be a strong support in favor of the alternative
419 network model (H_B) (*Kass and Raftery, 1995*).

420 **Evaluating INoDS performance**

421 We evaluated the accuracy of the in estimating the unknown transmission parameter β , and its
422 robustness to missing data was evaluated. To do so we first constructed a dynamic synthetic
423 network using the following procedure. At time-step $t = 0$, a static network of 100 nodes, mean
424 degree 4, and Poisson degree distribution was generated using the configuration model (*Molloy
425 and Reed, 1995*). At each subsequent time-step, 10% of edge-connections present in the previous
426 time-step were permuted, for a total of 100 time-steps. Next, through the synthetic dynamic
427 network, we performed 10 independent SI disease simulations with per contact rate of infection
428 transmission 0.01 to 0.1. Model accuracy was determined by comparing the estimated transmission
429 parameter, β , with the true transmission rate β^* that was used to perform disease simulations.
430 Since the synthetic network dataset did not contain any missing data, model accuracy was also
431 tested by evaluating the deviation of the estimated error parameter ϵ , from the expected value of
432 zero.

433 We also tested robustness of the tool in establishing the epidemiological relevance of a hypothesized
434 contact network against three potential sources of error in data-collection: missing nodes,
435 missing edges, and missing cases. The three scenarios of missing data were created by randomly
436 removing 10-95% of nodes, edges or infection cases from the simulated dataset described above.
437 True positive rate was calculated as the proportion of times the hypothesized contact network
438 model with missing data was correctly distinguished as statistically significant from an ensemble
439 of null networks generated by randomizing its edge connections. We calculated the true negative
440 rate as the proportion of times a network with the same degree distribution as the contact network
441 hypothesis, but randomized edge connections, was correctly classified as statistically insignificant.

442 Next, we compared INoDS with two previous approaches (k -test and network position test) that
443 have been used to establish an association between infection spread and contact network in a
444 host population. The k -test procedure involves estimating the mean infected degree (i.e., number
445 of direct infected contacts) of each infected individual in the network, called the k -statistic. The
446 p -value in the k -test is calculated by comparing the observed k -statistic to a distribution of null
447 k -statistics which is generated by randomizing the node-labels of infection cases in the network
448 (*VanderWaal et al., 2016*). Network position test compares the degree of infected individuals to that

449 of uninfected individuals (*Godfrey et al., 2009, 2010; MacIntosh et al., 2012*). The observed network
450 is considered to be epidemiologically relevant when the difference in average degree between
451 infected and uninfected individuals exceeds (at 5% significance level) the degree difference in an
452 ensemble of randomized networks.

453 **Applications to empirical data-sets**

454 We demonstrate the applications of our approach using two datasets from the empirical literature.
455 The first dataset comprises of dynamic networks of bee colonies (N = 5-7 individuals), where edges
456 represent direct physical contacts that were recorded using a color-based video tracking software.
457 A bumble bee colony consists of a single queen bee and infertile workers. Here, we focus on the
458 infection experiments in two colonies where infection was artificially introduced through a randomly
459 selected forager (colony UN1 and UN2). Infection progression through the colonies was tracked by
460 daily screening of individual feces, and the infection timing was determined using the knowledge of
461 the rate of replication of *C. bombi* within its host intestine.

462 The second dataset monitors the spread of the commensal bacterium *Salmonella enterica* in two
463 separate wild populations of the Australian sleepy lizard *Tiliqua rugosa*. The two sites consisted of 43
464 and 44 individuals respectively, and these represented the vast majority of all resident individuals at
465 the two sites (i.e., no other individuals were encountered during the study period). Individuals were
466 fitted with GPS loggers and their locations were recorded every 10 minutes for 70 days. Salmonella
467 infections were monitored using cloacal swabs on each animal once every 14 days. Consequently,
468 the disease data in this system do not identify the onset of each individual's infection. We used
469 a SIS (susceptible-infected-susceptible) disease model to reflect the fact that sleepy lizards can
470 be reinfected with salmonella infections. Proximity networks were constructed by assuming a
471 contact between individuals whenever the location of two lizards was recorded to be within 14m
472 distance of each other (*Leu et al., 2010*). The dynamic networks at both sites consisted of 70
473 static snapshots, with each snapshot summarizing a day of interactions between the lizards. We
474 constructed two contact network hypotheses to explain the spread of salmonella. The first contact
475 network hypothesis placed binary edges between lizards if they were ever within 14m distance
476 from each other during a day. The second contact network assigned edge weights proportional to
477 the number of times two lizards were recorded within 14m distance of each other during a day.
478 Specifically, edge weights between two lizards were equal to their frequency of contacts during a
479 day normalized by the maximum edge weight observed in the dynamic network.

480 **Acknowledgments**

481 This work was supported by the National Science Foundation Ecology and Evolution of Infectious
482 Diseases Grant 1216054. STL was supported by an Australian Research Council DECRA fellowship
483 (DE170101132), and an ARC grant to CM Bull (DP130100145), which funded the lizard project. We
484 thank Peter Majoros, Tom Haley, Alienor Quiblier and Ben Westwood for their assistance with lizard
485 fieldwork, and David Gordon for his lab work.

486 **Competing interests**

487 The authors declare that no competing interests exist.

488 **References**

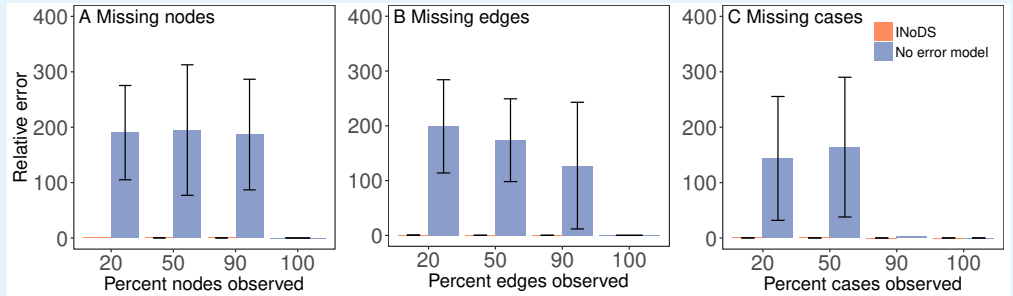
- 489 **Aiello CM**, Nussear KE, Esque TC, Emblidge PG, Sah P, Bansal S, et al. Host contact and shedding patterns
490 clarify variation in pathogen exposure and transmission in threatened tortoise *Gopherus agassizii*
491 : implications for disease modeling and management. *Journal of Animal Ecology*. 2016; p. n/a-n/a. <http://doi.wiley.com/10.1111/1365-2656.12511>, doi: 10.1111/1365-2656.12511.
492
- 493 **Antonovics J**, Wilson AJ, Forbes MR, Hauffe HC, Kallio ER, Leggett HC, et al. The evolution of transmission
494 mode. *Philosophical Transactions of the Royal Society B: Biological Sciences*. 2017; 372:20160083. doi:
495 10.1098/rstb.2016.0083.

- 496 **Aplin LM**, Farine DR, Morand-Ferron J, Cole EF, Cockburn A, Sheldon BC. Individual personalities predict
497 social behaviour in wild networks of great tits (*Parus major*). *Ecology Letters*. 2013; 16(11):1365–1372. doi:
498 [10.1111/ele.12181](https://doi.org/10.1111/ele.12181).
- 499 **Bansal S**, Grenfell BT, Meyers LA. When individual behaviour matters: homogeneous and network models
500 in epidemiology. *Journal of the Royal Society, Interface / the Royal Society*. 2007 oct; 4(16):879–91. doi:
501 [10.1098/rsif.2007.1100](https://doi.org/10.1098/rsif.2007.1100).
- 502 **Bansal S**, Read J, Pourbohloul B, Meyers LA. The dynamic nature of contact networks in infectious disease
503 epidemiology. *Journal of Biological Dynamics*. 2010; 4(5):478–489. doi: [10.1080/17513758.2010.503376](https://doi.org/10.1080/17513758.2010.503376).
- 504 **Bull CM**, Godfrey SS, Gordon DM. Social networks and the spread of *Salmonella* in a sleepy lizard population.
505 *Molecular Ecology*. 2012; 21(17):4386–4392. doi: [10.1111/j.1365-294X.2012.05653.x](https://doi.org/10.1111/j.1365-294X.2012.05653.x).
- 506 **Chen S**, White BJ, Sanderson MW, Amrine DE, Ilany A, Lanzas C. Highly dynamic animal contact network and
507 implications on disease transmission. *Scientific reports*. 2014; 4:4472. doi: [10.1038/srep04472](https://doi.org/10.1038/srep04472).
- 508 **Craft ME**. Infectious disease transmission and contact networks in wildlife and livestock. *Philosophical
509 Transactions of the Royal Society of London Series B, Biological Sciences*. 2015; 370(1669):1–12. doi:
510 [10.1098/rstb.2014.0107](https://doi.org/10.1098/rstb.2014.0107).
- 511 **Craft ME**, Caillaud D. Network models: An underutilized tool in wildlife epidemiology? *Interdisciplinary
512 Perspectives on Infectious Diseases*. 2011 jan; 2011:676949. doi: [10.1155/2011/676949](https://doi.org/10.1155/2011/676949).
- 513 **Cross PC**, Creech TG, Ebinger MR, Heisey DM, Irvine KM, Creel S. Wildlife contact analysis: emerging methods,
514 questions, and challenges. *Behavioral Ecology and Sociobiology*. 2012 jul; 66(10):1437–1447. [http://link.
515 springer.com/10.1007/s00265-012-1376-6](http://link.springer.com/10.1007/s00265-012-1376-6), doi: [10.1007/s00265-012-1376-6](https://doi.org/10.1007/s00265-012-1376-6).
- 516 **Danon L**, Ford AP, House T, Jewell CP, Keeling MJ, Roberts GO, et al. Networks and the epidemiology of
517 infectious disease. *Interdisciplinary perspectives on infectious diseases*. 2011 jan; 2011:284909. doi:
518 [10.1155/2011/284909](https://doi.org/10.1155/2011/284909).
- 519 **Eames K**, Bansal S, Frost S, Riley S. Six challenges in measuring contact networks for use in modelling. *Epidemics*.
520 2015; 10:72–77. doi: [10.1016/j.epidem.2014.08.006](https://doi.org/10.1016/j.epidem.2014.08.006).
- 521 **Farine D**. The dynamics of transmission and the dynamics of networks. *Journal of Animal Ecology*. 2017;
522 86(3):415–418. doi: [10.1111/1365-2656.12659](https://doi.org/10.1111/1365-2656.12659).
- 523 **Farine DR**, Whitehead H. Constructing, conducting, and interpreting animal social network analysis. *The Journal
524 of animal ecology*. 2015; (July):1144–1163. doi: [10.1111/1365-2656.12418](https://doi.org/10.1111/1365-2656.12418).
- 525 **Fefferman NH**, Ng KL. How disease models in static networks can fail to approximate disease in dynamic net-
526 works. *Physical Review E - Statistical, Nonlinear, and Soft Matter Physics*. 2007; 76(3):1–11. doi: [10.1103/Phys-
527 RevE.76.031919](https://doi.org/10.1103/PhysRevE.76.031919).
- 528 **Fenner AL**, Godfrey SS, Michael Bull C. Using social networks to deduce whether residents or dispersers
529 spread parasites in a lizard population. *Journal of Animal Ecology*. 2011; 80(4):835–843. doi: [10.1111/j.1365-
2656.2011.01825.x](https://doi.org/10.1111/j.1365-
530 2656.2011.01825.x).
- 531 **Foreman-Mackey D**, Hogg DW, Lang D, Goodman J. emcee: The MCMC Hammer. *Publications of the Astronom-
532 ical Society of the Pacific*. 2013; 125(925):306–312. doi: [10.1086/670067](https://doi.org/10.1086/670067).
- 533 **Franz M**, Nunn CL. Network-based diffusion analysis: a new method for detecting social learning. *Proc Biol Sci*.
534 2009; 276(1663):1829–1836. doi: [10.1098/rspb.2008.1824](https://doi.org/10.1098/rspb.2008.1824).
- 535 **Godfrey SS**. Networks and the ecology of parasite transmission: A framework for wildlife parasitol-
536 ogy. *International journal for parasitology Parasites and wildlife*. 2013 dec; 2(1):235–245. doi:
537 [10.1016/j.ijppaw.2013.09.001](https://doi.org/10.1016/j.ijppaw.2013.09.001).
- 538 **Godfrey SS**, Bull CM, James R, Murray K. Network structure and parasite transmission in a group living
539 lizard, the gidgee skink, *Egernia stokesii*. *Behavioral Ecology and Sociobiology*. 2009; 63(7):1045–1056. doi:
540 [10.1007/s00265-009-0730-9](https://doi.org/10.1007/s00265-009-0730-9).
- 541 **Godfrey SS**, Moore JA, Nelson NJ, Bull CM. Social network structure and parasite infection patterns in a territorial
542 reptile, the tuatara (*Sphenodon punctatus*). *International Journal for Parasitology*. 2010; 40(13):1575–1585.
543 doi: [10.1016/j.ijpara.2010.06.002](https://doi.org/10.1016/j.ijpara.2010.06.002).

- 544 **Groendyke C**, Welch D, Hunter DR. Bayesian inference for contact networks given epidemic data. *Scandinavian*
545 *Journal of Statistics*. 2011; 38(3):600–616.
- 546 **Hamede RK**, Bashford J, McCallum H, Jones M. Contact networks in a wild Tasmanian devil (*Sarcophilus*
547 *harrisii*) population: using social network analysis to reveal seasonal variability in social behaviour and its
548 implications for transmission of devil facial tumour disease. *Ecology letters*. 2009 nov; 12(11):1147–57. doi:
549 [10.1111/j.1461-0248.2009.01370.x](https://doi.org/10.1111/j.1461-0248.2009.01370.x).
- 550 **Jennions M**, Møller A. A survey of the statistical power of research in behavioral ecology and animal behavior.
551 *Behavioral Ecology*. 2003; 14(3):438–445. doi: [10.1093/beheco/14.3.438](https://doi.org/10.1093/beheco/14.3.438).
- 552 **Johnson PCD**, Barry SJE, Ferguson HM, Müller P. Power analysis for generalized linear mixed models in ecology
553 and evolution. *Methods in Ecology and Evolution*. 2015; 6(2):133–142. doi: [10.1111/2041-210X.12306](https://doi.org/10.1111/2041-210X.12306).
- 554 **Kass R**, Raftery A. Bayes Factors. *Journal of the American Statistical Association*. 1995; 90(430):773–795. doi:
555 [10.1080/01621459.1995.10476572](https://doi.org/10.1080/01621459.1995.10476572).
- 556 **Krause J**, Krause S, Arlinghaus R, Psorakis I, Roberts S, Rutz C. Reality mining of animal social systems. *Trends in*
557 *ecology & evolution*. 2013 sep; 28(9):541–51. doi: [10.1016/j.tree.2013.06.002](https://doi.org/10.1016/j.tree.2013.06.002).
- 558 **Lartillot N**, Philippe H. Computing Bayes Factors Using Thermodynamic Integration. *Systematic Biology*. 2006;
559 55(2):195–207. doi: [10.1080/10635150500433722](https://doi.org/10.1080/10635150500433722).
- 560 **Leu ST**, Kappeler PM, Bull CM. Refuge sharing network predicts ectoparasite load in a lizard. *Behavioral ecology*
561 *and sociobiology*. 2010 sep; 64(9):1495–1503. doi: [10.1007/s00265-010-0964-6](https://doi.org/10.1007/s00265-010-0964-6).
- 562 **MacIntosh AJJ**, Jacobs A, Garcia C, Shimizu K, Mouri K, Huffman Ma, et al. Monkeys in the middle: para-
563 site transmission through the social network of a wild primate. *PloS one*. 2012 jan; 7(12):e51144. doi:
564 [10.1371/journal.pone.0051144](https://doi.org/10.1371/journal.pone.0051144).
- 565 **Manlove KR**, Cassirer EF, Plowright RK, Cross PC, Hudson PJ. Contact and contagion: Probability of transmission
566 given contact varies with demographic state in bighorn sheep. *Journal of Animal Ecology*. 2017; 86(4):908–920.
567 doi: [10.1111/1365-2656.12664](https://doi.org/10.1111/1365-2656.12664).
- 568 **Molloy M**, Reed B. A Critical Point for Random Graphs With a Given Degree Sequence. *Random Structures and*
569 *Algorithms*. 1995; 6(2-3):161–180.
- 570 **Newman MEJ**. Spread of epidemic disease on networks. *Physical Review E - Statistical, Nonlinear, and Soft*
571 *Matter Physics*. 2002; 66(1):1–11. doi: [10.1103/PhysRevE.66.016128](https://doi.org/10.1103/PhysRevE.66.016128).
- 572 **Otterstatter MC**, Thomson JD. Contact networks and transmission of an intestinal pathogen in bumble bee
573 (*Bombus impatiens*) colonies. *Oecologia*. 2007 nov; 154(2):411–21. doi: [10.1007/s00442-007-0834-8](https://doi.org/10.1007/s00442-007-0834-8).
- 574 **Pellis L**, Ball F, Bansal S, Eames K, House T, Isham V, et al. Eight challenges for network epidemic models.
575 *Epidemics*. 2014; 10:58–62. doi: [10.1016/j.epidem.2014.07.003](https://doi.org/10.1016/j.epidem.2014.07.003).
- 576 **Robert C**, Casella G. *Monte Carlo Statistical Methods*. Springer Texts in Statistics; 2004.
- 577 **Rohani P**, Zhong X, King AA. Contact Network Structure Explains the Changing Epidemiology of Pertussis.
578 *Science*. 2010; 330(6006):982–985. doi: [10.1126/science.1194134](https://doi.org/10.1126/science.1194134).
- 579 **Sah P**, Leu ST, Cross PC, Hudson PJ, Bansal S. Unraveling the disease consequences and mechanisms of modular
580 structure in animal social networks. *Proceedings of the National Academy of Sciences of the United States of*
581 *America*. 2017 apr; 114(16):4165–4170. doi: [10.1073/pnas.1613616114](https://doi.org/10.1073/pnas.1613616114).
- 582 **Sah P**, Mann J, Bansal S. Disease implications of animal social network structure: a synthesis across social
583 systems. *Journal of Animal Ecology*. 2017; .
- 584 **Sah P**, Nussear KE, Esque TC, Aiello CM, Hudson PJ, Bansal S. Inferring social structure and its drivers from
585 refuge use in the desert tortoise, a relatively solitary species. *Behavioral Ecology and Sociobiology*. 2016; p.
586 1–13. doi: [10.1007/s00265-016-2136-9](https://doi.org/10.1007/s00265-016-2136-9).
- 587 **Shirley MDF**, Rushton SP. The impacts of network topology on disease spread. *Ecological Complexity*. 2005;
588 2(3):287–299. doi: [10.1016/j.ecocom.2005.04.005](https://doi.org/10.1016/j.ecocom.2005.04.005).
- 589 **Silk MJ**, Jackson AL, Croft DP, Colhoun K, Bearhop S. The consequences of unidentifiable individuals for the
590 analysis of an animal social network. *Animal Behaviour*. 2015; 104:1–11. doi: [10.1016/j.anbehav.2015.03.005](https://doi.org/10.1016/j.anbehav.2015.03.005).

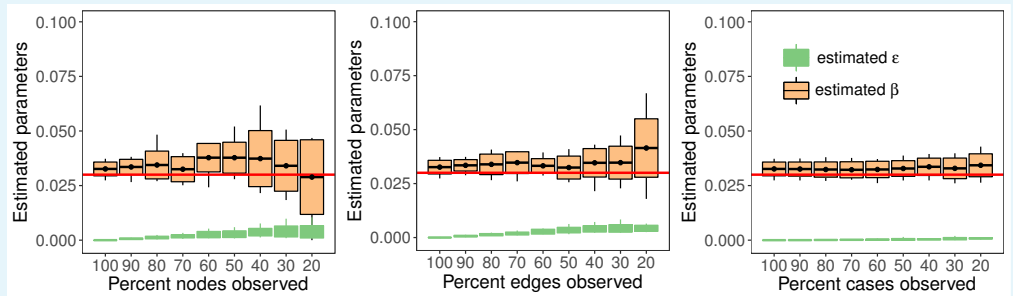
- 591 **Stack JC**, Bansal S, Anil Kumar VS, Grenfell B. Inferring population-level contact heterogeneity from common
592 epidemic data. *Journal of the Royal Society, Interface / the Royal Society*. 2013; 10(78):20120578. doi:
593 [10.1098/rsif.2012.0578](https://doi.org/10.1098/rsif.2012.0578).
- 594 **Tanner MA**, Wong WH. The Calculation of Posterior Distributions by Data Augmentation: Rejoinder. *Journal of*
595 *the American Statistical Association*. 1987; 82(398):548–550. doi: 10.2307/2289463.
- 596 **VanderWaal K**, Enns EA, Picasso C, Packer C, Craft ME. Evaluating empirical contact networks as potential
597 transmission pathways for infectious diseases. *Journal of The Royal Society Interface*. 2016; 13(121):20160166.
598 doi: [10.1098/rsif.2016.0166](https://doi.org/10.1098/rsif.2016.0166).
- 599 **Velthuis aGJ**, Bouma A, Katsma WEa, Nodelijk G, De Jong MCM. Design and analysis of small-scale
600 transmission experiments with animals. *Epidemiology and infection*. 2007; 135(2):202–217. doi:
601 [10.1017/S095026880600673X](https://doi.org/10.1017/S095026880600673X).
- 602 **Volz E**, Meyers LA. Susceptible-infected-recovered epidemics in dynamic contact networks. *Proceedings of the*
603 *Royal Society B: Biological Sciences*. 2007; 274(1628):2925–2934. doi: [10.1098/rspb.2007.1159](https://doi.org/10.1098/rspb.2007.1159).
- 604 **Welch D**, Bansal S, Hunter DR. Statistical inference to advance network models in epidemiology. *Epidemics*.
605 2011; 3(1):38–45. doi: [10.1016/j.epidem.2011.01.002](https://doi.org/10.1016/j.epidem.2011.01.002).
- 606 **White LA**, Forester JD, Craft ME. Using contact networks to explore mechanisms of parasite transmission in
607 wildlife. *Biological Reviews*. 2015; <http://doi.wiley.com/10.1111/brv.12236>, doi: [10.1111/brv.12236](https://doi.org/10.1111/brv.12236).

608 **Appendix 1**



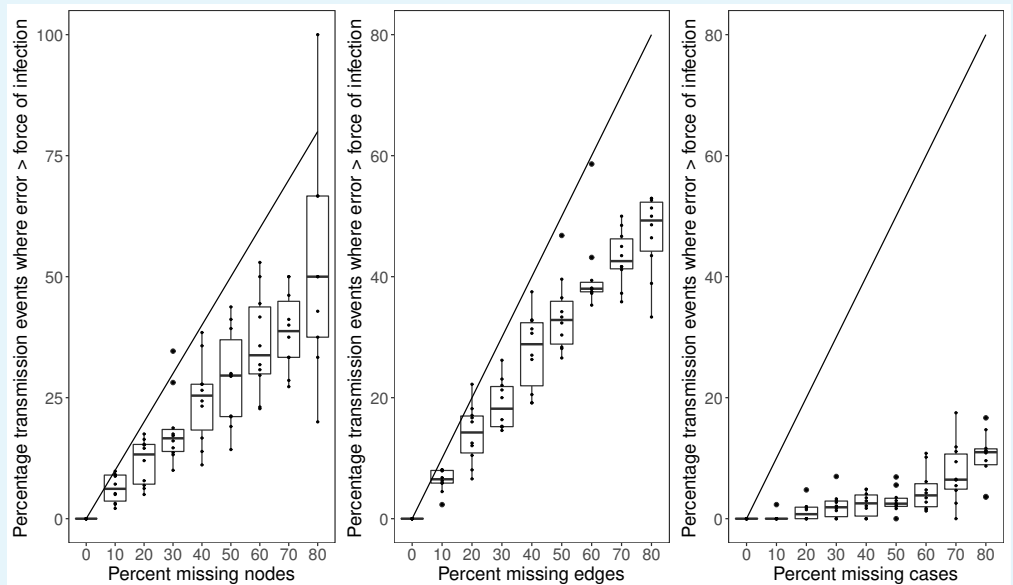
609
610
611
612
613
614
616

Appendix 1 Figure 1. Relative error in the estimations of parameter β under missing data conditions with and without the inclusion of the error parameter (ϵ) in the INoDS formulation. The simulated infectious disease spread (SI model, per contact transmission rate pathogen = 0.03) was performed on static network with 100 nodes, Poisson degree distribution, and a average degree of 3. Relative error was calculated as $\frac{\beta - \beta'}{\beta}$, where β is the per contact transmission rate of the simulated pathogen (=0.03) and β' is the value of social transmission parameter estimated



617
618
619
620
621
622
623
624
625
626

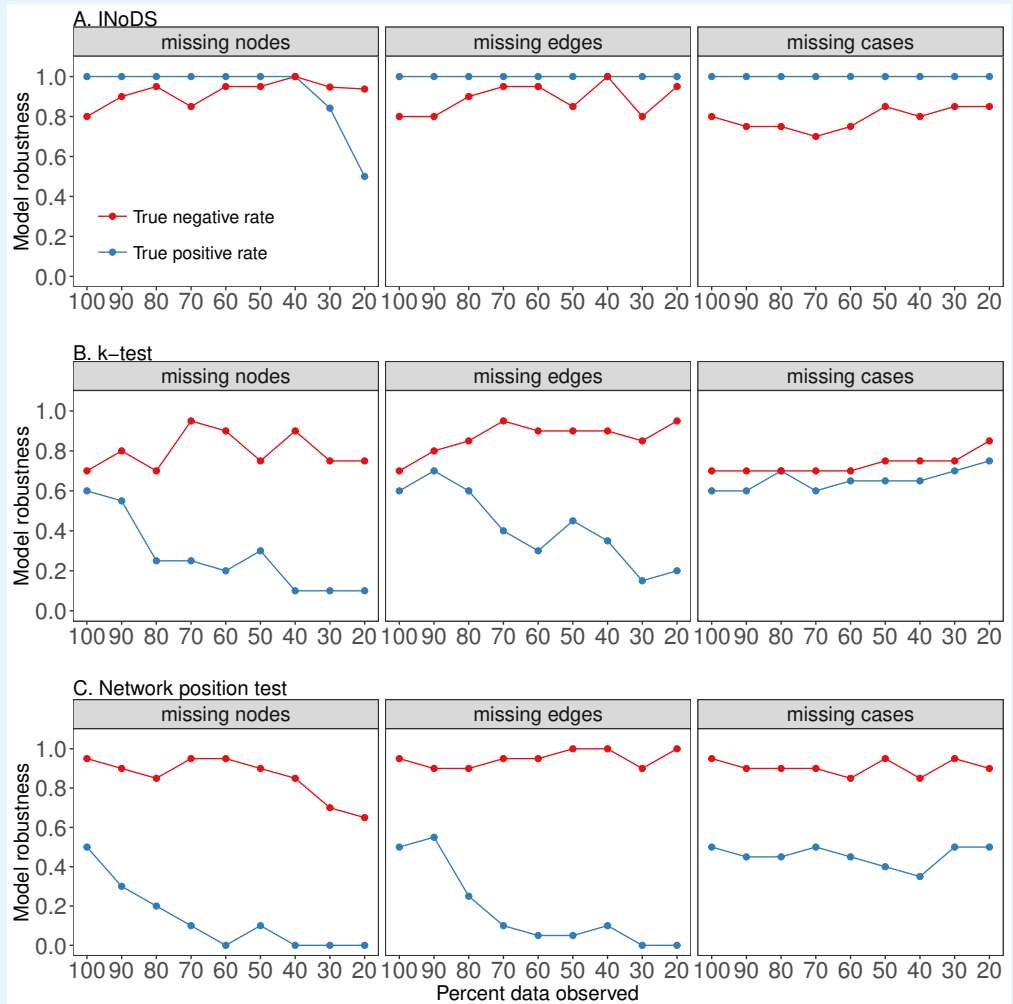
Appendix 1 Figure 2. Estimation of per contact transmission rate (β) and the error parameter (ϵ) by INoDS under three forms of missing data conditions - (A) missing nodes, (B) missing edges and (C) missing infection cases. Simulations of susceptible-infected (SI) model of infectious disease spread were performed on static network with 100 nodes, Poisson degree distribution, and an average degree of 3. Each boxplot summarizes the results of 10 independent disease simulations; the horizontal line in the middle is the mean of estimated parameter values, the top and the bottom horizontal line is the standard deviation, and the tip of the vertical line represents the maximum/minimum value. The solid red line represents the true value of β used in the disease simulations. Since the simulations were performed on a known synthetic network, the expected value of error parameter is zero.



628

629
630
631
632
633
635

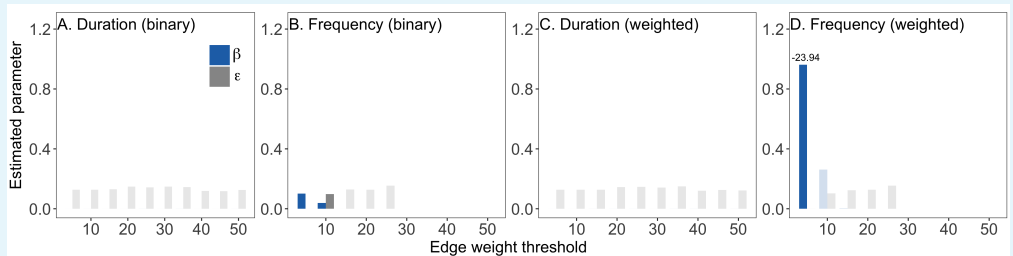
Appendix 1 Figure 3. Relationship between error ϵ and force of infection ($=\beta w_i(t-1)$) with increasing percentage of missing data. Each boxplot summarizes the results of 10 independent disease simulations (indicated by points); the horizontal line in the middle is the mean percent transmission events where the asocial force is greater than the infection force contributed by the social connections. The top and the bottom horizontal line is the standard deviation, and the tip of the vertical line represents the maximum/minimum value.



636
637
638
639
640
641
642
643
645

Appendix 1 Figure 4. Plot of sensitivity and specificity of (A) INoDS, (B) k -test and (C) network position test to three common forms of missing data - missing nodes, missing edges and missing infection cases. The observed network in this case is a static network with 100 nodes, Poisson degree distribution and a mean network degree of 3. Simulations of pathogen spread with per contact transmission rate of 0.03 were performed through the observed static network. Null expectation in INoDS and network position test was generated by permuting the edge connections of the observed networks, creating an ensemble of null networks. In k -test, the location of infection cases within the observed network are permuted, creating a permuted distribution of k -statistic (VanderWaal et al., 2016)

646



647 **Appendix 1 Figure 5.** Identifying the contact network model of *Crithidia* spread in bumble bee colony
648 (colony UN2). Edges in the contact network models represent physical interaction between the bees.
649 Since the networks were fully connected, a series of filtered contact networks were constructed by
650 removing weak weighted edges in the network. The x-axis represents the edge weight threshold that
651 was used to remove weak edges in the network. Two types of edge weights were tested - duration and
652 frequency of contacts. In addition, across all ranges of edge weight threshold, the weighted networks
653 were converted to binary networks. The results shown are estimated values of the per contact rate of
654 infection transmission β , and estimated values of error ϵ , for the (A-B) two types of binary network, (C)
655 contact duration weighted network, (D) contact frequency weighted network. The faded bars
656 correspond to networks where β parameter is statistically insignificant. Numbers above bars indicate
657 the log Bayesian (marginal) evidence of the networks that were detected to have statistically significant
658 higher predictive power as compared to an ensemble of null networks ($P < 0.05$, corrected for multiple
659 comparisons). We note that frequency networks with more than 25% weak edge removed failed to
660 converge in (C) and (D), and therefore the transmission parameter associated with these contact
662 networks were not estimated.

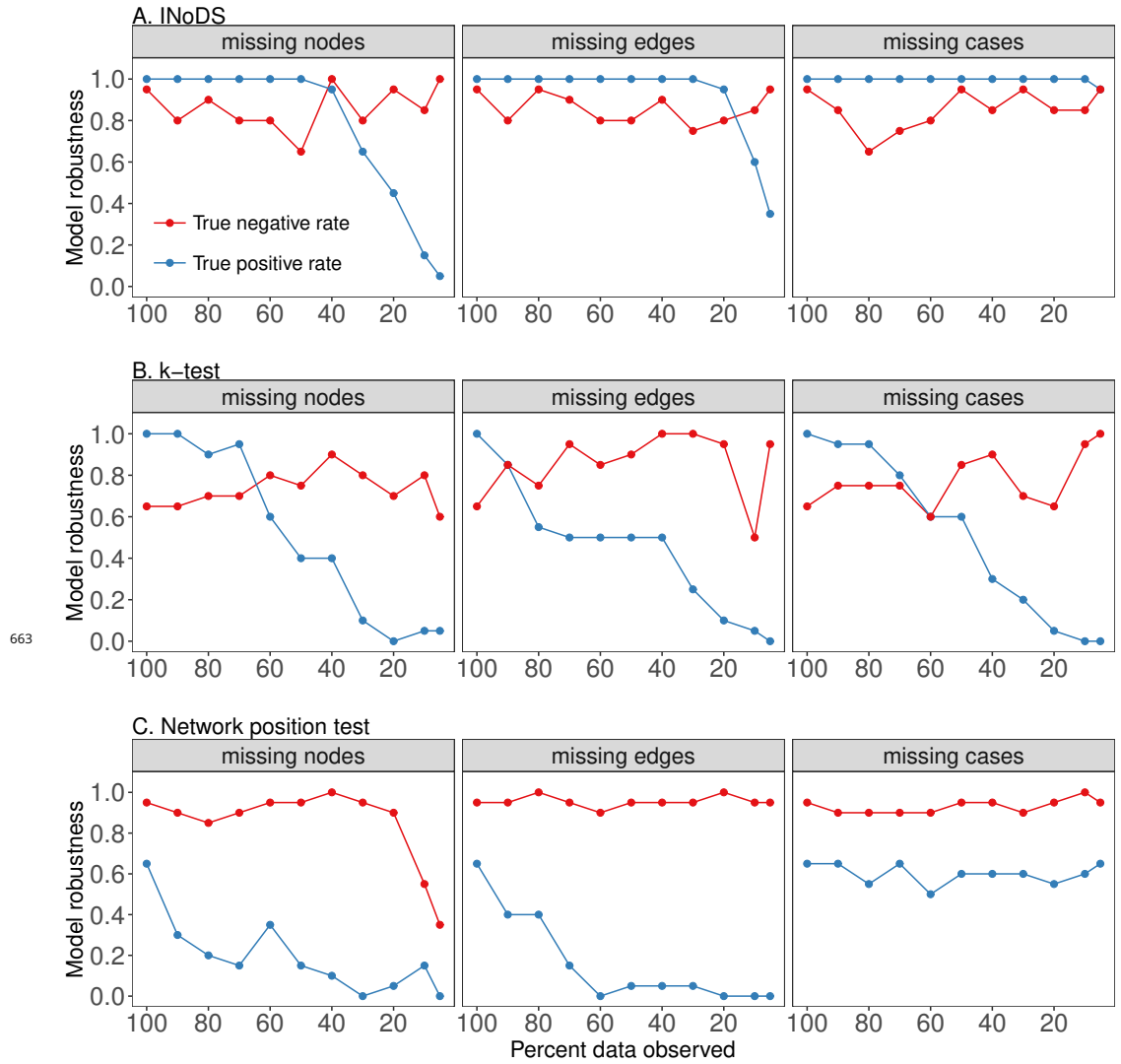


Figure 3-Figure supplement 1. Robustness plot of (A) INoDS, (B) k -test and (C) network position test to three common forms of missing data - missing nodes, missing edges and missing infection cases. The null expectation in INoDS and the network position test was generated by permuting network edges, creating an ensemble of null networks. In the k -test, the location of infection cases within the observed network are permuted, creating a permuted distribution of the k -statistic (VanderWaal et al., 2016).